

# Three-Dimensional Image Reconstruction Of Human Finger Joints

Alexander D. Klose, Rong Song, Alexander K. Scheel†, Uwe Netz\*, Jürgen Beuthan\*, and Andreas H. Hielscher

*Departments of Biomedical Engineering and Radiology, Columbia University  
MC 8904, 500 West 120th Street, New York, NY 10027, USA*

*Email: ak2083@columbia.edu*

†*Departments of Nephrology and Rheumatology, Georg-August University,  
Robert-Koch-Strasse 40, D-37075 Göttingen, Germany*

\* *Institute for Medical Physics and Laser Medicine,  
Free University of Berlin, Germany*

**Abstract:** We have developed a three-dimensional image reconstruction algorithm to recover the spatial distribution of optical properties in human finger joints for early diagnosis and monitoring of rheumatoid arthritis. An optimization method iteratively employs a light propagation model based on the equation of radiative transfer for recovering the unknown absorption and scattering coefficient distribution for near-infrared light inside the joint tissue. We show three-dimensional image reconstruction results of finger joints and compare them to two-dimensional images of previous studies.

© 2005 Optical Society of America

**OCIS codes:** (170.3010) image reconstruction techniques, (170.3660) light propagation in tissue, (170.5280) photon migration, (170.6960) tomography, (100.3190) inverse problems.

## 1 Introduction

In previous studies we have demonstrated the application of two-dimensional (2D) sagittal tomographic imaging of human *proximal interphalangeal* (PIP) joints [1, 2] using the equation of radiative transfer (ERT) as light propagation model. We were able to differentiate between healthy and rheumatoid conditions of joints by using reconstructed 2D maps of the absorption and scattering coefficients. However, the image reconstructions were limited to a 2D sagittal tissue slice and did not account for the three-dimensional (3D) tissue volume. To further improve on the promising clinical results obtained with 2D models and to potentially increase sensitivity and specificity, we have developed a 3D transport-theory-based image reconstruction scheme for reconstructing the optical parameters of PIP joints and compared the results to 2D images.

## 2 Methods

Our 3D image reconstruction technique is a nonlinear optimization approach for finding the unknown volume distribution of optical parameters [3]. A forward model for light transport based on the ERT predicts the detector readings on the tissue boundary for a given initial distribution of absorption and scattering coefficients. An objective function  $\varphi$  is defined that is a  $\chi^2$ -error norm of the predicted and measured detector readings. This objective function is minimized by iteratively updating an initial optical parameter distribution along a search direction. The optimization process is finished after the measured and predicted data match and a minimum of the objective function is found. The final distribution of absorption and scattering coefficients is displayed in an image.

The light distribution originating from a source positioned at the outer boundary of a finger joint can be described by the time-independent ERT for the radiance  $\psi(\mathbf{r}, \boldsymbol{\Omega})$  at spatial position  $\mathbf{r}$  and direction  $\boldsymbol{\Omega}$

$$\boldsymbol{\Omega} \cdot \nabla \psi + (\mu_a + \mu_s) \psi = \mu_s \int_{4\pi} p(\boldsymbol{\Omega}, \boldsymbol{\Omega}') \psi(\boldsymbol{\Omega}') d\boldsymbol{\Omega}' \quad (1)$$

with scattering coefficient  $\mu_s$  and absorption coefficient  $\mu_a$ . The scattering phase function  $p(\boldsymbol{\Omega}, \boldsymbol{\Omega}')$  is described by the Henyey-Greenstein function and takes the anisotropic scattering behavior of biological tissue

into account. The boundary condition for the ERT consists of partially reflected light, due to the refractive index mismatch, and of boundary sources  $S(\mathbf{\Omega}, \mathbf{r})$  at  $\mathbf{r} \in \partial V$ . It is given by

$$\psi(\mathbf{r}, \mathbf{\Omega}) = S(\mathbf{r}, \mathbf{\Omega}) + R(|\mathbf{\Omega}' \cdot \mathbf{n}|)\psi(\mathbf{r}, \mathbf{\Omega}') \quad (2)$$

for all  $\mathbf{n} \cdot \mathbf{\Omega} < 0$  at  $\partial V$ . The direction  $\mathbf{\Omega}'$  points outward  $\mathbf{\Omega}' = \mathbf{\Omega} - 2(\mathbf{\Omega} \cdot \mathbf{n})\mathbf{n}$  for all  $\mathbf{n} \cdot \mathbf{\Omega}' > 0$  at  $\partial V$ . The reflectivity  $R$  is given with

$$R(\cos \vartheta') = \frac{1}{2} \left( \frac{n_m \cos \vartheta'' - n_0 \cos \vartheta'}{n_m \cos \vartheta'' + n_0 \cos \vartheta'} \right)^2 + \frac{1}{2} \left( \frac{n_m \cos \vartheta' - n_0 \cos \vartheta''}{n_m \cos \vartheta' + n_0 \cos \vartheta''} \right)^2, \quad (3)$$

where the angle of incidence  $\vartheta'$  from within the medium with refractive index  $n_m$  is given by  $\cos \vartheta' = \mathbf{\Omega}' \cdot \mathbf{n}$ . The refracted angle  $\vartheta''$  in the outside medium (air) with  $n_0 = 1$  satisfies *Snell's law*  $n_m \sin \vartheta' = n_0 \sin \vartheta''$ . The critical angle  $\vartheta'_c$  for total internal reflection is given by  $n_m \sin \vartheta'_c = n_0$ .

We solve the ERT with a *source iteration* method based on a *finite-difference discrete-ordinates* discretization [4]. The direction  $\mathbf{\Omega}$  is replaced with a set of discrete ordinates  $\mathbf{\Omega}_k$  with full level symmetry. The spatial derivatives are substituted with finite difference approximations defined on a structured *Cartesian* grid. We are using a *blocking-off region* method for taking curved tissue geometries into account. In this approach the physical domain is modeled using a so-called *nominal domain*. A nominal domain is divided into two regions. First, the active region is that part of the physical domain where the solution is sought. Second, the inactive region lies outside the physical boundary, hence, all Cartesian grid points are blocked-off.

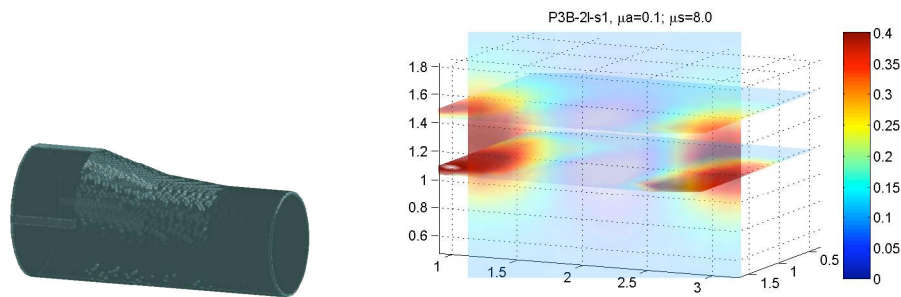
The spatial distribution of the optical parameters is reconstructed by applying a limited-memory Broyden-Fletcher-Goldfarb-Shanno (BFGS) technique to an objective function  $\varphi(\mu)$  that describes the difference between the measured,  $m_d$ , and predicted data,  $p_d$ . The predicted detector readings  $p_d$  at the boundary are derived from the numerical solution given by the partial current  $J$ . We minimize the objective function and the final result is the distribution of the optical parameters. The BFGS method requires the gradient of the objective function,  $d\varphi/d\mu$ , which is calculated by means of an adjoint differentiation technique. More details can be found, for example, in Klose *et al* [3].

### 3 Experimental results

We have performed tomographic measurements on human PIP joints using near-infrared light at wavelength  $\lambda = 678$  nm. Using the measurement data we reconstructed  $\mu_s$  and  $\mu_a$  by employing a Cartesian grid of a finger joint model. Therefore, we have developed a 3D numerical joint model that is composed of four conical cylinders with an elliptical cross-section mimicking the curved surface geometry of a human finger (Fig. 1(a)). The finger joint model had a plane posterior side and an oblique interior side. All grid points enclosed by the finger surface of the model are defined on a structured *Cartesian* grid with spatial separation  $\Delta x = \Delta y = \Delta z = 0.05$  cm between adjacent grid points. Furthermore, the spatial dimensions of the numerical model are defined by the thickness  $a$  and circumference  $U$  at three different distinct points of the human finger. These points coincide with the three intersections of all four conical cylinders of the numerical model. The elliptical cross-sections of the model are determined by the two,  $b$  and  $a$ , axis of the ellipse. The short axis  $a$  was given by the sagittal thickness of the joint, as provided by the physician. The long axis  $b$  could be calculated from the circumference  $U$  and the short axis  $a$  of the ellipse. The length of the numerical model was 4 cm with the PIP joint at the center. Hence, we obtained a Cartesian grid with approximately 200,000 grid points depending on the spatial discretization  $\Delta x$ ,  $\Delta y$ , and  $\Delta z$  and the actual physical dimensions of the finger. The measurement data were collected from PIP joints of healthy volunteers with a joint imaging system as introduced by Hielscher *et al* [1]. A laser diode illuminated the interior side of the PIP joint at 11 different positions with a spatial separation of 0.2 cm. A silicon diode measured the transmitted light on the posterior side of the joint at 16 different positions with a spatial separation of 0.2cm. The source-detector configuration yielded  $D = 11 \times 16$  measurement points, which became subsequently input to the 3D reconstruction algorithm.

The reconstructed scattering and absorption coefficients show clearly the synovial fluid in the center of the images. For example, Fig. 1(b) shows the 3D reconstruction of absorption coefficient, with the smallest value

at  $\mu_a = 0.01 \text{ cm}^{-1}$  inside the cavity. The adjacent tissue parts to the left and to the right in the image depict bones, which show absorption coefficients of approximately  $\mu_a = 0.4 \text{ cm}^{-1}$ . That is 20–40% higher than what we found by using a 2D reconstruction algorithm, as can be seen in Figs. 1(c) and 1(d). Fig. 1(c) shows a sagittal slice of the 3D reconstruction of  $\mu_a$ , whereas Fig. 1(d) shows a  $\mu_a$  reconstruction using only a 2D model. We also observe that the spatial distribution of  $\mu_a$  differs slightly between images generated by the 2D and 3D codes. Similar results were found for images of  $\mu_s$ . Further studies involving patients with RA are under way to determine if these differences indeed improve the diagnostic value of this method. This work was supported in part by a grant from the National Institute of Arthritis Musculoskeletal and Skin Diseases (NIAMS-2R01-AR046255), which is part of the National Institutes of Health.



(a) 3D PIP joint model

(b) 3D reconstruction of  $\mu_a$  of human PIP joint, joint cavity is seen at the center with small values of  $\mu_a$